18èmes Journées Internationales de Thermique (JITH 2017)
Monastir (Tunisie), 25 - 27 Octobre 2017

Brownian motion Effect on the Flow and Heat Transfer of Nanofluids Over a Backward-Facing Step

Lotfi BOUAZIZI[a] and Saïd TURKI [b]

[a,b] Laboratory of Computational Fluid Dynamics and Transfer Phenomena, National Engineering School of Sfax,
[a] Department of Mechanical, National Engineering School of Sfax, BP W-3038, 1173 Sfax, Tunisia
[b] Faculty of Sciences of Sfax, Department of Physics, BP 1171, 3000 Sfax, Tunisia
lot.bouazizi@yahoo.fr
said.turki@fss.rnu.tn

Abstract - A numerical investigation was conducted to analyze the effect of Brownian motion on the flow field and the heat transfer over a backward-facing step using nanofluids. The computations were done for a various type of nanoparticles (CuO, Al_2O_3 and ZnO) dispersed in a base fluid (water), volume fraction of nanoparticles φ in the range of 1% to 6% at a fixed Reynolds number $Re = 450$, Prandtl number $Pr = 6.2$ and nanoparticle diameter $d_{np} = 30$ nm. Results show that the Brownian motion contribution leads to a reduction in the size of the primary recirculation zone as well as the reattachment length. The Brownian motion could be an important factor that enhances the thermal conductivity of nanofluids, resulting then to the improvement in heat transfer at the channel walls. Enhancement in the maximum value of Nu of 29% and 26% are obtained at the lower and the upper walls of the channel, respectively, compared to the one obtained without Brownian motion. On the other hand, results show a marked improvement in heat transfer compared to the base fluid, this improvement is more pronounced, on the upper wall, for higher φ.

Keywords: nanofluids, thermal conductivity, Brownian motion, backward-facing step, heat transfer

1. Introduction

It is well known that the study of backward-facing step flows is an important branch of fundamental fluid mechanics. Since the publication of Armaly's et al. [1] work, several studies have been conducted in this area using pure fluid. However, to the best of our knowledge, few research studies have tackled this area using nanofluids. This new class of fluids, composed of metal nanoparticles suspended in a base fluid, has recently appeared, due to their anomalous thermal conductivity enhancement and many studies (Ramsak and Skerget [2], Tinney and Ukeiley [3] and Abu-mawleh [4] ….) have been undertaken in the area of flow and heat transfer of nanofluids, showing that these new fluids have a remarkable power of heat exchange compared to conventional liquid. This enhanced thermal behavior of nanofluids could provide a basis for an enormous innovation for heat transfer intensification, which is a major importance to a number of industrial sectors including transportation, power generation, heating, cooling, ventilation and air-conditioning, …etc. Abu-Nada [5] was notably the pioneer to analyze the effect of nanofluids on the flow pattern and its related heat transfer over a backward-facing step. Results, obtained in forced convection, show that nanoparticles with high thermal conductivity have more enhancement on the value of Nusselt number outside the recirculation zones. The effect of nanofluids flow on a mixed convection heat transfer over a $2D$ horizontal micro scale backward-facing step placed in a duct has been conducted numerically by Kherbeet et al. [6]. Their results, obtained for different nanoparticles (Al_2O_3, CuO, SiO_2 and ZnO) with volume fractions in the range of 1– 4% and nanoparticles diameter ranging from 25nm to 70nm, show that the Nusselt number increases with the increase of the volume fraction and Reynolds number. Mohammed et al. [7] studied the heat transfer enhancement of $2D$ laminar and turbulent mixed convective flows adjacent to backward facing step with baffle installation onto the channel wall using different types of nanofluids. Their results show that SiO_2 gives the highest Nusselt number and velocity distribution followed by Al_2O_3, ZnO and CuO respectively, while pure water is the lowest. In addition, they showed that the Nusselt number increased with increasing the volume fraction and decreased with increasing the diameter of the nanoparticles. The optimum position of the baffle installation for heat transfer enhancement varies with the specified thermal and flow conditions and the effects of baffle widths and baffle numbers on heat transfer are insignificant. Hussein Togun

[8] studied numerically the forced convection of laminar nanofluid flow and heat transfer over a backward-facing step with and without obstacle. He showed that the Nusselt number increases with increasing in Reynolds number and the height of the rectangular cylinder. The biggest thermal augmentation was found for Reynolds number of 225, height of the rectangular cylinder of 4.5 mm, and 4 % of volume fractions of CuO nanoparticles.

The present work contributed to the knowledge of flow and heat transfer enhancement for many industrial applications. It deals with $2D$ combined convective flow over a backward-facing step with a built in adiabatic square cylinder by using different types of nanoparticles such as CuO, Al_2O_3 and ZnO dispersed in a base fluid (water). Our study is particularly focused on the effect of the Brownian motion on the flow field and its related heat transfer. Numerical simulations are performed out for different nanoparticles volume fraction ranging from 0 to 6% at a fixed Reynolds number $Re = 450$, Prandtl number $Pr = 6.2$ and nanoparticle diameter $d_{np} = 30$ nm.

2. Governing equations

Both of the flow geometry and the coordinate system are shown in Fig. 1, with a blockage ratio in $1/4$. The dimensionless of the continuity, momentum and thermal energy equations governing the laminar flow over the backward-facing step can be written in the following conservative form:

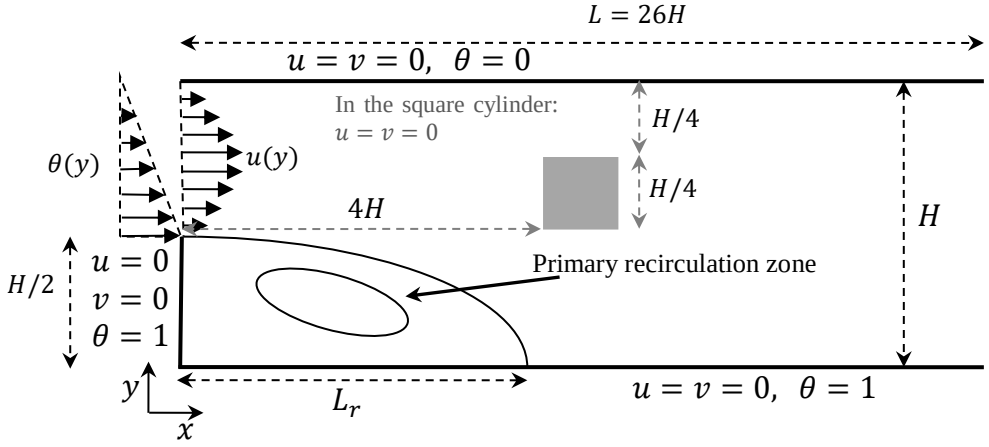

Figure 1. Configuration definition

$$div(\boldsymbol{V}) = 0 \tag{1}$$

$$\frac{\partial u}{\partial \tau} + div(\boldsymbol{J_u}) = -\frac{\rho_f}{\rho_{nf}}\frac{\partial P}{\partial x}, \qquad \boldsymbol{J}_u = u\boldsymbol{V} - \frac{1}{Re}\frac{\mu_{nf}}{\mu_f}\frac{\rho_f}{\rho_{nf}}\boldsymbol{grad}(u) \tag{2}$$

$$\frac{\partial v}{\partial \tau} + div(\boldsymbol{J_v}) = -\frac{\rho_f}{\rho_{nf}}\frac{\partial P}{\partial y} + \frac{\varphi\rho_s\beta_s + (1-\varphi)\rho_f\beta_f}{\rho_{nf}\beta_f}Ri\theta, \qquad \boldsymbol{J}_v = v\boldsymbol{V} - \frac{1}{Re}\frac{\mu_{nf}}{\mu_f}\frac{\rho_f}{\rho_{nf}}\boldsymbol{grad}(v) \tag{3}$$

$$\frac{\partial \theta}{\partial \tau} + div(\boldsymbol{J_\theta}) = 0, \qquad \boldsymbol{J}_\theta = \theta\boldsymbol{V} - \frac{1}{Re.Pr}\frac{\alpha_{nf}}{\alpha_f}\boldsymbol{grad}(\theta) \tag{4}$$

The effective density (ρ_{nf}), the thermal expansion coefficient (β_{nf}) and heat capacitance $(\rho Cp)_{\mathrm{nf}}$ of the nanofluids are defined as (Khanafer et al. [9]):

$$\rho_{nf} = (1-\varphi)\rho_f + \varphi\rho_s \tag{5}$$

$$\beta_{nf} = (1-\varphi)\,\beta_f + \varphi\beta_s \tag{6}$$

$$(\rho Cp)_{nf} = (1-\varphi)\,(\rho Cp)_f + \varphi(\rho Cp)_s \tag{7}$$

Table 1 shows the thermophysical properties of water and various nanoparticles.

Table 1: The thermo-physical properties of water and different nanoparticles
At $T = 300K$ (Incropera F. P. and DeWitt D. P. [10])

Thermo-physicalproperties	$Water$	Al_2O_3	CuO	ZnO
Density, $\rho\ (kg/m^3)$	998.2	3970	6500	5600
Specificheat, $c_p\ (J/kg.K)$	4182	765	535.6	495.2
Thermal conductivity, $k\ (W/m\ K)$	0.6	40	20	13
Dynamic viscosity, $\mu\ (Ns/m^2)$	0.001003	--	--	--
Thermal expansion, $\beta\ (1/K)$	207E-06	5.80E-06	4.30E-06	4.31E-06

Vajjha et al. [11] proposed that the effective thermal conductivity is composed of the particle's conventional static part and a Brownian motion part. This two-component thermal conductivity model takes into account the effects of particle size, particle volume fraction and temperature dependence as well as types of particle and base fluid combinations. From their experimental data, they proposed a correlation which was a combination of the static part proposed long ago by Maxwell and a dynamic part due to the Brownian motion of nanoparticles.

$$k_{nf} = k_{static} + k_{Brownian} \tag{8}$$

The k_{static} is the static thermal conductivity based on Maxwell classical correlation.

$$k_{static} = k_f \left[\frac{(k_s+2k_f)-2\varphi(k_f-k_s)]}{(k_s+2k_f)+\varphi(k_f-k_s)}\right] \tag{9}$$

where $k_s$and $k_f$are the thermal conductivities of the solid particles and the base fluid respectively.
The thermal conductivity due to the Brownian motion is given by Vajjha et al. [11] as:

$$k_{Brownian} = 5\times10^4\beta\varphi\rho c_{p,f}\sqrt{\frac{KT}{\rho_{nf}\mathrm{d}_{np}}}f(T,\varphi) \tag{10}$$

Where

$$f(T,\varphi) = (2.8217\times10^{-2}\varphi + 3.917\times10^{-3})\left(\frac{T}{T_0}\right) + (-3.0669\times10^{-2}\varphi - 3.91123\times10^{-3}) \tag{11}$$

K is the Boltzmann constant, T is the fluid temperature, and T_0 is the reference temperature.

The viscosity of the nanofluid is approximately considered as viscosity of a base fluid if containing dilute suspension of fine spherical particles. Masoumi et al. [12] developed a theoretical model for the prediction of the effective viscosity of nanofluids based on Brownian motion. They showed that their model could accurately predict the effective viscosity of different nanofluids. It is expressed as follow:

$$\mu_{nf} = \mu_f + \frac{\rho_{np}V_B d_{np}^2}{72C\delta} \tag{12a}$$

in which:

$$V_B = \frac{1}{\mathrm{d}_{np}}\sqrt{\frac{18KT}{\pi\rho_{np}\mathrm{d}_{np}}} \tag{12b}$$

$$\delta = \sqrt[3]{\frac{\pi}{6\varphi}}\mathrm{d}_{np} \tag{12c}$$

$$C = \mu_f^{-1}\left[\left(c_1\mathrm{d}_{np}\times10^9 + c_2\right)\varphi + \left(c_3\mathrm{d}_{np}\times10^9 + c_4\right)\right] \tag{12d}$$

where:

$c_1 = -0.000001133$
$c_2 = -0.000002771$
$c_3 = 0.00000009$
$c_4 = -0.000000393$

$\mu_{nf}$and μ_f are the viscosity of nanofluid and base fluid respectively, d_{np} is the nanoparticle diameter and φ is the nanoparticle volume fraction.
The β equations for Al_2O_3, ZnO and CuO particles are expressed in Table 2 as it is given by Vajjha R.S and Das D. K. [13].

Table 2: Curve-fit relations for proposed by Vajjha R.S and Das D. K. [13]

Type of particles	β	Concentration	Temperature
Al_2O_3	$8.4407(100\varphi)^{-1.07304}$	$1\% \leq \varphi \leq 10\%$	$298\ K \leq T \leq 363\ K$
ZnO	$8.4407(100\varphi)^{-1.07304}$	$1\% \leq \varphi \leq 7\%$	$298\ K \leq T \leq 363\ K$
CuO	$9.8810(100\varphi)^{-0.9446}$	$1\% \leq \varphi \leq 6\%$	$298\ K \leq T \leq 363\ K$

Koo and Kleinstreuer [14] further investigated laminar nanofluid flow in micro heat sinks using the effective nanofluid thermal conductivity model. For the effective viscosity due to micro mixing in suspensions, they proposed:

$$\mu_{nf} = \mu_{static} + \mu_{Brownian} = \mu_{static} + \frac{k_{Brownian}}{k_f} \times \frac{\mu_f}{Pr} \tag{13}$$

where $\mu_{static} = \frac{\mu_f}{(1-\varphi)^{2.5}}$ is viscosity of the nanofluid, as given originally by Brinkman [15] and the value of Prandtl number maintained at $Pr = 6.2$.

In the above equations, the space coordinates, velocities, time and pressure are normalized with the downstream channel height H, the maximum velocity of the channel inlet u_0, the characteristic time $\frac{H}{u_0}$ and the characteristic pressure $\rho_f u_0^2$ respectively. The dimensionless variable θ was defined as: $\theta = \frac{(T-Tc)}{(Th-Tc)}$ where T_h and T_c are hot and cold temperatures respectively.

Boundary condition

No-slip boundary conditions for velocities on all the solid walls were used. The temperature at the upper wall of the channel is constant and equal to T_c, corresponding to $\theta = 0$. The step and the lower walls of the channel are assumed to be isothermally heated at T_h, corresponding to $\theta = 1$.

At the channel inlet, a normal component of velocity is assumed to be zero and a fully developed parabolic profile for the axial velocity, expressed by $u(y) = -16(y^2 - 1.5y + 0.5)$, is deployed. The temperature of the incoming stream is assumed to be linear and expressed by Abu-nada [5]: $\theta(y) = 2(1-y)$.

At the channel exit, the convective boundary condition, given by $\frac{\partial \phi}{\partial t} + u_{av}\frac{\partial \phi}{\partial x} = 0$, is used where the variable ϕ is the dependent variable (u, v, θ) and u_{av} is the mean channel inlet velocity. It is noted here that, as mentioned by Sohankar et al. [16] and Abbassi et al. [17], the convective boundary condition reduces the number of iterations per time step and allows a shorter downstream computational domain when compared to the case of the Neumann boundary condition. The square cylinder walls are specified as adiabatic.

The thermal heat flux exchanged between the flow and the horizontal walls of backward-facing step is characterized by the space averaged Nusselt number evaluated as follows:

$$Nu_{av} = \frac{1}{L}\int_0^L Nu(x)dx \tag{14}$$

Where *Nu*(*x*) is the local Nusselt number, computed with the following equation (Abu-Nada [5]):

$$Nu(x) = \frac{1}{\theta_b(x)-1}\frac{k_{nf}}{k_f}\frac{\partial \theta}{\partial y}\Big|_{wall} \tag{15}$$

$\theta_b(x)$is the bulk temperature, calculated using the velocity and the temperature distribution with the equation:

$$\theta_b(x) = \frac{\int_0^1 u\theta dy}{\int_0^1 u dy} \tag{16}$$

The time and space-averaged Nusselt number at the horizontal walls of backward-facing step $< \overline{Nu} >$ is evaluated as follows:

$$< \overline{Nu} > = \frac{1}{\tau_2 - \tau_1}\int_{\tau_1}^{\tau_2} Nu_{av} d\tau \tag{17}$$

where the time interval $(\tau_2 - \tau_1)$ is large compared to the period of oscillations and usually chosen as an integer multiple of period oscillations.

3. Solution procedures

The combined continuity, momentum and energy equations are solved using a finite volume method of Patankar [18], where the control volume cells for velocity components are staggered with respect to the main

control volume cells. This use of a staggered grid prevents the occurrence of checker board pressure fields. The convection terms in equations (2-4) were discretized using hybrid scheme, while the diffusion terms were discretized using second order central scheme. The SIMPLER algorithm was applied to solve the pressure-velocity coupling in conjunction with an alternating direction implicit scheme to perform the time evolution.

Our computations were achieved using 366×119 non uniform meshes with a variable grid sizes $10^{-2} \leq \Delta x \leq 10^{-1}$ and $10^{-3} \leq \Delta y \leq 10^{-2}$. In order to study the grid independence, one case was run with 561×255 grid points with $5.10^{-3} \leq \Delta x \leq 7.10^{-2}$ and $5.10^{-4} \leq \Delta y \leq 5.10^{-3}$ for $Re = 450$, $Pr = 6.2$, $Ri = 0$ and $\varphi = 0$ (pure water). The computation results show a difference of only 1.5%, 0.7% and 1.1% in the values of the reattachment length Lr, the time andspace averaged Nusselt numbers $< \overline{Nu} >$ at the lower and the upper walls of the channel respectively. Since the computation time with 561×255 grids is nearly four times higher than that with 366×119 grids, we decided to cancel it and carry out that of the 366×119 grids.

The present computational procedure has been validated by comparing the predicted reattachment length and averaged Nusselt number with the results of Abu-Nada [5] obtained in laminar forced convection flow of $Cu - water$ nanofluid over a backward-facing step without square cylinder. Figures 2 and 3 show that the present results are in good agreement with those found by Abu-Nada [5]. The maximum deviations are of only about 3% and 2.7% for the reattachment length and the averaged Nusselt number respectively. We can therefore conclude that our computational code can predict correctly the flow and heat transfer of nanofluids over abackward-facing step.

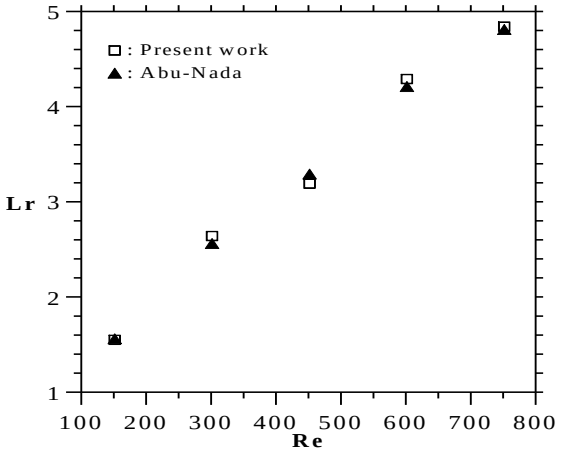

Figure 2. Comparison of reattachment length results with those obtained by Abu-Nada at φ = 0.

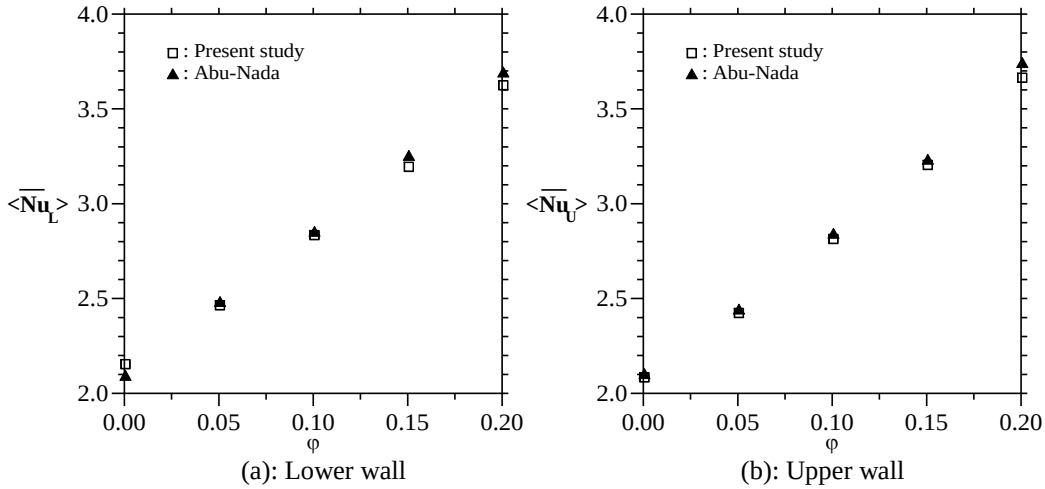

(a): Lower wall (b): Upper wall

Figure 3. Comparison of time and space-averaged Nusselt number results with those obtained by Abu-Nada at *Re* = 450 ($Water/Cu$).

For all the investigated cases in this paper, the computational time step used is equal to $\Delta\tau = 0.005$. A time step of $\Delta\tau = 0.0025$ does not cause any change on the numerical results.

4. Results and discussions

A numerical simulation has been done to study the effect of the Brownian motion of nanoparticles on fluid flow and heat transfer over abackward-facing step. Thus, the main objective of this study is to examine the heat transfer enhancement of $2D$ laminar and mixed convective flow adjacent to backward facing step with and without adiabatic square cylinder using different types of nanofluids. Computations were carried out for a $CuO - water$, $Al_2O_3 - water$ and $ZnO - water$ nanofluids flow over a backward-facing step under temperature difference ΔT up to 35, volume fraction φ ranging from 0 to 0.06 when the Reynolds number is kept constant at $Re = 450$. Here, the effects of Brownian motion, types of nanoparticles and presence of square cylinder on several parameters are presented. These parameters are reattachment length, velocity, streamlines, temperature distribution, isotherms and Nusselt number .

The first part concerns the verification of the model of Brownian motion for the separated fluid flow with nanoparticles and the influence of Brownian motion on the heat transfer in the backward-facing step without square cylinder. The flow separates from the step edge because of a sudden expansion of the duct and impinges onto the downstream wall. The flow is divided into two parts: one move in the opposite direction towards the step wall and forms the recirculation region and the other moves downstream from the step. A reattachment zone lies between them, where the velocity has zero value (Armaly's et al. [1]), and the location of the impingement of the separating streamline onto the lower wall is called the reattachment point (see Fig. 1). The flow is characterized by recirculating vortices and flow reversals within the separation bubble. The effects of the nanoparticles and Brownian motion on the reattachment length are shown in Fig. 4. The results were presented for steady regime and $\Delta T = 0$ represent the forced convection. It is observed that the reattachment length starts to drop with increase in solid volume fraction. This is due to the relatively less inertia effect at higher solid volume fraction. Also, the reattachment length was influenced by the Brownian motion, especially for higher nanoparticles volume fraction. This can be explained, as well that, by the increase of the dynamic viscosity of the nanofluid with the increase of φ (see equation 13) and hence the friction forces on the edge of the step walls increase. These forces tend to oppose to the development of the primary recirculation zone (see Fig. 5). This behavior may be caused by the generation of a vortex located at the tip of the primary recirculation zone as shown in Fig. 5. This vortex which grows in size with time leaves the primary recirculation zone toward the main flow. In the case of flow without Brownian motion, Lr decreases slightly with increasingφ. The type of nanofluid has no significant effect on the reattachment length. With Brownian motion, the great reattachment length corresponds with to nanofluid at a low density, i.e. Al_2O_3, ZnO then CuO. This reduction is in the vicinity of 7% and 64% in cases without and with Brownian motion, respectively, for a concentration of 0.06.

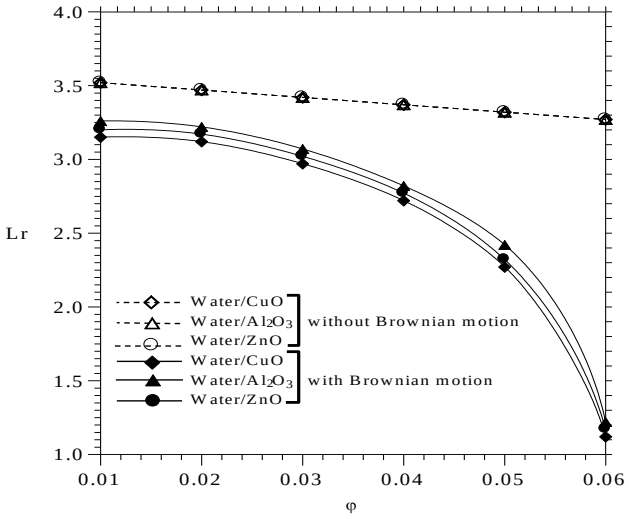

Figure 4. Effect of Brownian motion on variation of Lr with nanoparticles volume fraction φ

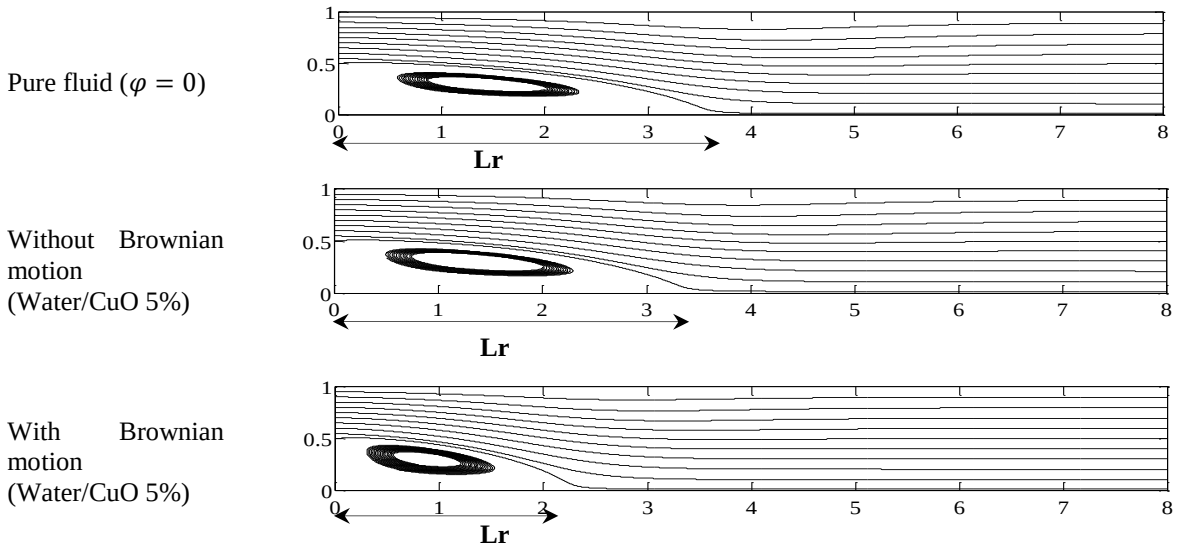

Figure 5. Effect of Brownian motion on streamlines for Water/CuO nanofluid

The velocity profile of a base fluid with CuO nanoparticles, with and without Brownian motion, at $X = 2$ along the stepped wall is shown in Fig. 6(b). The flow is separated as the flow passed through the edge of the step due to the sudden geometry expansion. It is shown in Fig. 6(b) that, in with Brownian motion, at high buoyancy level the negative velocity profile increases in the recirculation region and the positive profile above the recirculation region increases as well. It is found that the size of the recirculation region increases as the temperature between the heated stepped wall and the nanofluid increases as shown in Fig. 6(a). This is because the expanded streamwise flow is affected by the buoyancy force which is acting perpendicular to it. Therefore, the buoyancy force is not more significant to push up the high velocity flow with lower temperature, but it affected the flow by increasing the reattachment length as indicated previously. At the downstream streamwise location of $X = 2$, the flow exhibits negative velocities adjacent to the heated wall, indicating that a recirculation region is developed downstream of the step. The velocity gradient is larger in the negative sense for the nanofluid without Brownian motion (i.e., the velocity gradient increases in the negative sense as the density of the nanofluid decreases when approaching the hot zone). Note that, the nanofluid with a higher density has a lower flow velocity as compared to the nanofluids of lower density. In fact, the density increases, by considering Brownian motion ($\mu_{nf} = \mu_{static} + \mu_{Brownian}$).

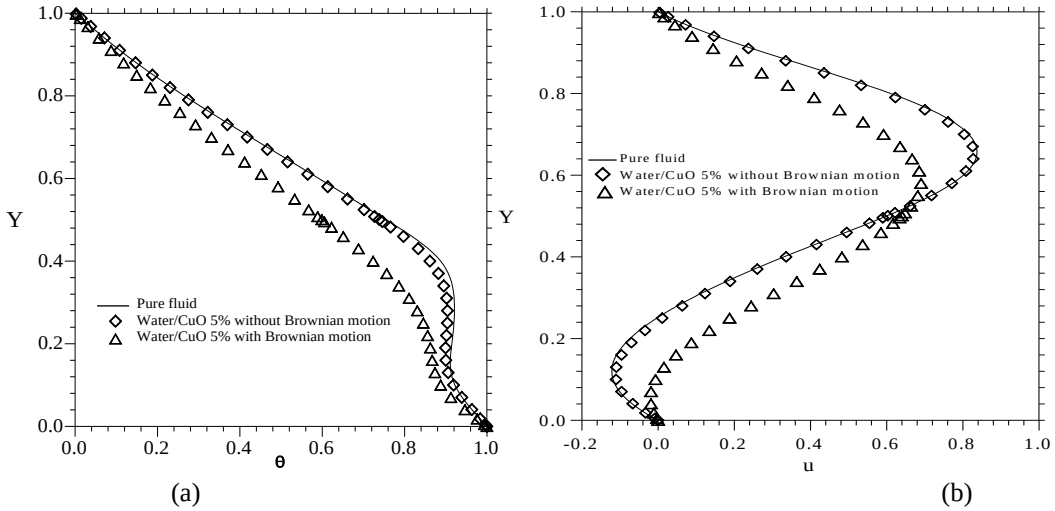

(a) (b)

Figure 6. Effect of Brownian motion for $\varphi = 0.05$of $X = 2$, (a) temperature distribution and (b) velocity distribution

Effects of adding nanoparticles on the isotherms are shown in Fig. 7. This figure indicates that the heat transfer rate and distortion of the isotherms are increased by adding nanoparticles to the base fluid. The thinning of thermal boundary layer, which is clearly observed in presence of nanoparticles, is the main reason for this behavior and so it increases Nusselt number. The temperature contours are much denser near the lower wall of the channel with Brownian motion. While Nusselt number is a multiplication of temperature gradient and the thermal conductivity ratio. Since, in presence of Brownian motion the increases in temperature gradient due to the presence of nanoparticles is much higher than without Brownian motion, therefore an enhancement in Nusselt number is occurred when considering the Brownian motion. The effect of primary recirculation is clearer on the isothermal, where the streamlines and isotherms have similar behavior and no significant difference was seen. It is also shown that the temperature contours are steeper for pure fluid in the near wake region.

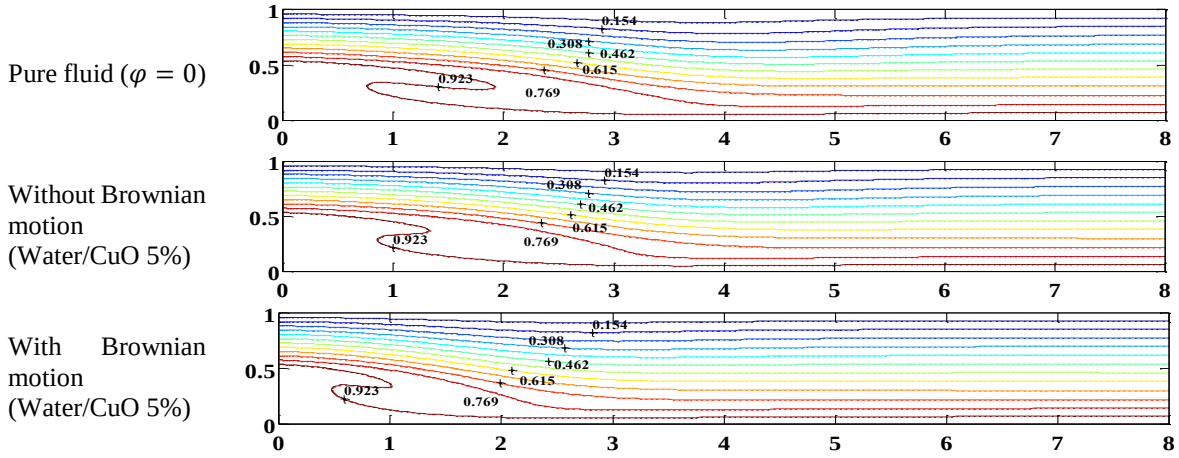

Figure 7. Effect of Brownian motion on isothermal lines contours

To study the effect of Brownian motion on heat transfer, a close glance at Fig. 8 presenting the averaged Nusselt number at the lower and the upper walls reveals a clear increase in the Nusselt number observed when increasing the nanoparticles volume fraction for different nanofluids, with and without Brownian motion. Furthermore, as shown in this figure, the heat transfer increases by considering the Brownian motion compared with that in the case of without Brownian motion. As it can be seen, the Brownian motion has a significant effect on heat transfer where there is an important enhancement except on the lower wall. For example, for $\varphi = 0.04$, an enhancement in the vicinity of 4.91%, 4.48% and 3.76%, for CuO, Al_2O_3 and ZnO, respectively. As we know, the Brownian motion is the random motion of nanoparticles suspended in the base fluid. Note that the Brownian motion of nanoparticles increases the thermal conductivity of nanofluid because the thermal conductivity of nanofluids is due to both the static and dynamic mechanisms. Also, Brownian motion of nanoparticles could contribute to the heat transfer augmentation by two mechanisms. These ways are motion of nanoparticles that transport heat energy, and the microconvection of fluid surrounding nanoparticles (valipoor [19]).

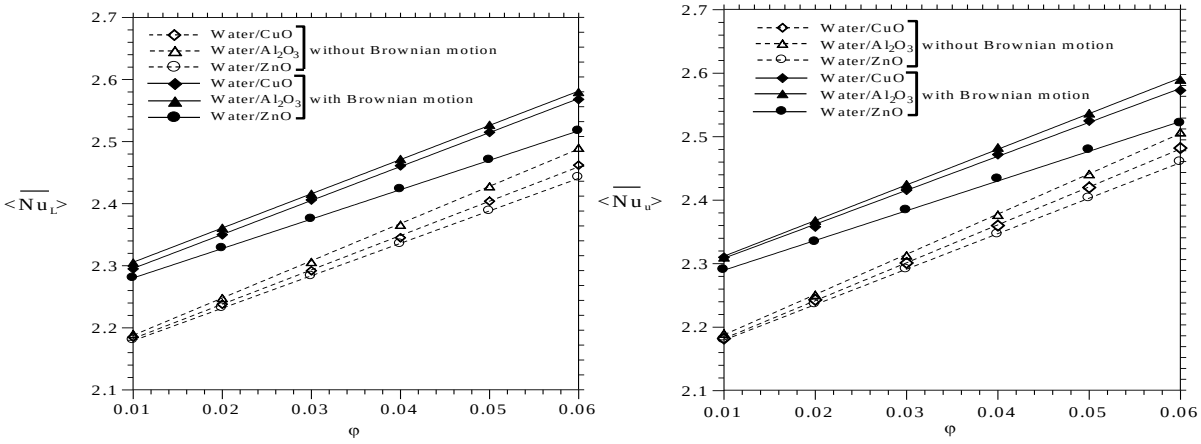

(a) : Lower wall (b) : Upper wall

Figure 8. Effect of Brownian motionon variation of $< \overline{Nu} >$ with φ

The effect of the Brownian motion and the nanoparticle type on the Nusselt number distribution along the downstream wall behind the backward-facing step is also studied as shown in Fig. 9. In this case three different

nanoparticles types were utilized CuO, Al_2O_3 and ZnO at $\varphi = 0.05$. It is observed that all these nanofluids produced higher results compared to pure water. For all the studied models, the Nusselt number is higher than that of the one obtained without taking the Brownian effects into account. It is clear that Al_2O_3 nanofluid has the highest Nusselt number, followed by CuO and ZnO respectively. As mentioned above, that by considering the Brownian motion, the nanofluid has a smaller recirculation region (see Fig. 12), and the reverse flow of the vortex mixes with the main separated flow closer to the wall of the backward-facing step. Kherbeet et al. [6], indicate that in this case, it's because the flow is found to have the highest peak maximum Nusselt number in the region. Also, results depict that, the maximum and the minimum of the local Nusselt number, which increases and moves towards at the inlet of channel by adding nanoparticles then by considering Brownian motion where the thermal conductivity increases. This can be explained by the fact that the thermal conductivity and specific heat capacity influence the flow along with density and viscosity. In Mohammed et al.'s work [20], for this reason, the peaks of nanofluids change as the flow changes its temperature (see Fig. 6). The Nusselt number increases until it reaches its optimal value. After that, the Nusselt number decreases due to the growth of temperature difference until it reaches the minimum value in the region where the recirculation flow joins the main separated flow. At the upper wall (Fig. 9 (b)), the Nusselt number decreased rapidly and reached to its minimum value near the point at the recirculation zone, and this due to the reduction of the temperature gradient. In fact, near the step region, fluid velocity and consequently, convection coefficient increases because of the sudden contraction in the flow domain thus leading to a reduction in the temperature difference between the wall and the nanofluid. So, more propagation of heat from the hot walls inside the flow domain which leads to development of temperature is achieved more rapidly at the flow under the influence of the recirculation to make returned vortices which decrease the temperature difference. The isothermal lines of nanofluids near the upper wall are become sparse (see for example Fig. 7 from $X = 2$ to $X = 4$). Therefore, a reduction of the temperature gradient and a reduction of the heat transfer are achieved in this zone at the upper wall. Another important result, is that the first recirculation zone, repulses streamlines from the upper wall to the lower wall as found by Abu-Nada [5]. At that point, the Nusselt number increases again due to the decrease of the temperature during the mixing until it reaches the point from that where the recirculation influence ends, the Nusselt number gradually decreases.

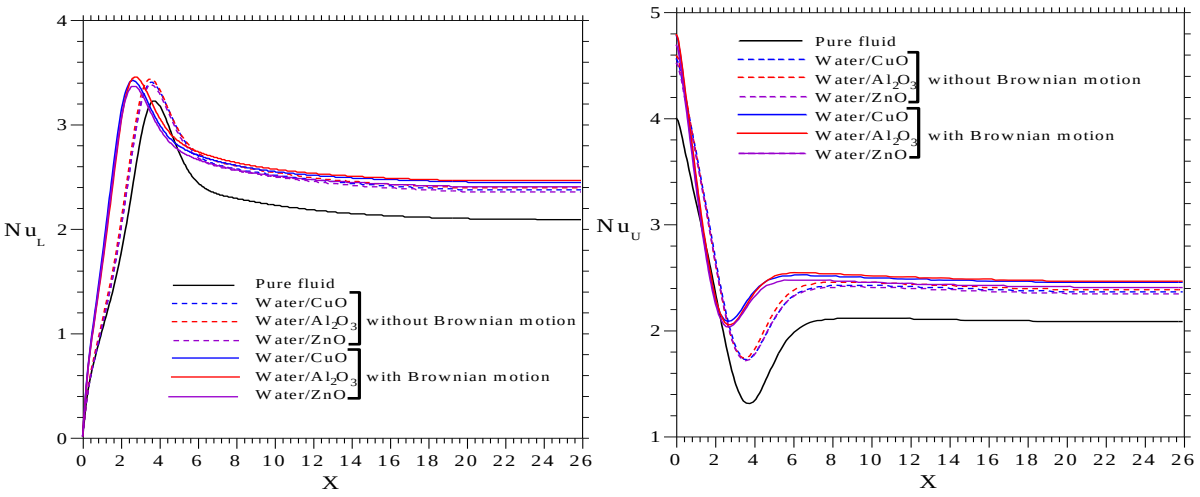

(b) : Lower wall (b) : Upper wall

Figure 9. Effect of Brownian motion on local Nusselt distribution for $\varphi = 0.05$

The second part is devoted to the study of heat transfer of nanofluid in channel sudden expansion in the presence of square cylinder. Figure 10 shows the axial variation of Nu along the lower and upper walls of the channel for $\varphi = 0.05$ with square cylinder for $Water/Al_2O_3$ nanofluid. The maximum value of Nu is detected at $X = 4$, corresponds to the front face of the square cylinder (see Fig. 11), where Nu reveals the appearance of peak where an enhancement in the Nusselt number is registered at the horizontals wall of BFS. The maximum value of Nu drops sharply to a very low value at the point of rear face of the square cylinder. This behavior can be explained by noting that the vortices increase dramatically inside the second recirculation zone, which tends to maximize viscous contribution to Nu in this zone. However, at the point of reattachment there are no shear stresses. This eliminates viscous contribution and leaves only the conduction contribution to Nu. This explains the sharp drop in Nu after reaching its maximum value. On the lower wall the minimum value of Nu occurs at $X = 0$, at the bottom left corner, since at this point there is no motion and no heat transfer is taking place. The reason for having a maximum value of Nu at the leading edge of the walls because of the presence of the square cylinder is due to the development of the viscous boundary layer, flow separation and high heat transfer rates where the highest

values of local Nusselt numbers are recorded at the leading edge of the walls. Figure 12 confirms this result where we have plotted the isotherm contours at different nanoparticles volume fraction for $Water/Al_2O_3$ nanofluid. In fact, the recirculation zone behind the step is compressed stronger in presence of square cylinder and the tightening of the isotherms near the horizontal walls is observed, compared to the case without square cylinder (see Fig. 7). It is reasonable with square cylinder, the heat transfer characteristics can be effectively improved as can be seen in Fig. 13.

Furthermore, Fig. 10(b) reveals the appearance of a second peak after the point of reattachment of the secondary recirculation bubble on the upper wall of the channel. Thus, it is very clear that this second peak is related to the secondary recirculation bubble. The secondary recirculation bubble does influence the value of Nuon the upper wall of the channel. However, its main influence is to narrow down the flow passage between the secondary bubble and the square cylinder, as shown in Fig. 11. This would increase velocity gradients between the secondary recirculation bubble and the square cylinder. These high values of velocity gradients at the wall are responsible for high rates of entropy generation numbers that cause the appearance of the second peak zone. Thus, it can be concluded that the effect of the secondary recirculation zone is crucial in increasing local rates of entropy generation on the upper wall of the channel and, accordingly, the total rates of entropy generation over the entire flow domain.

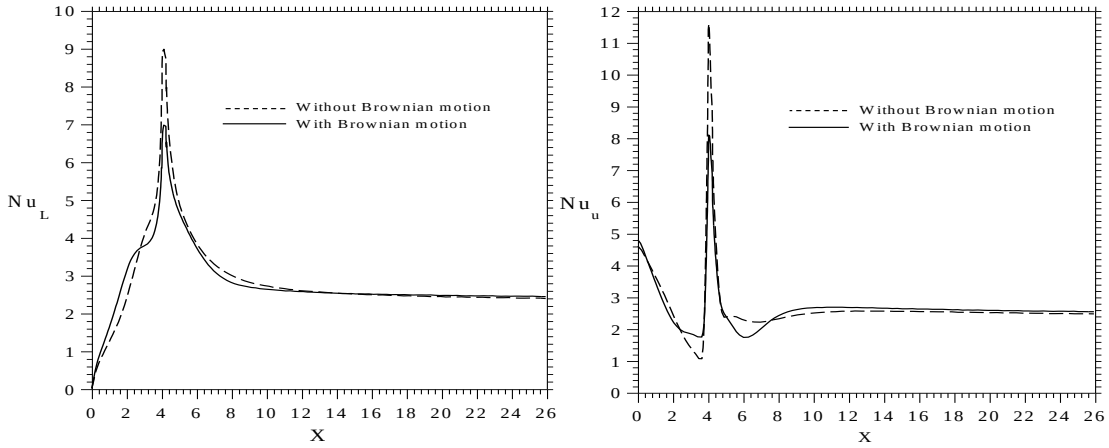

(a): Lower wall (b) : Upper wall

Figure 10. Local Nusselt distribution for $Water/Al_2O_3$ nanofluid for$\varphi = 0.05$ with square cylinder.

The results presented in Figs. 11 and 12 illustrate that the square cylinder, in presence of nanoparticles, could cause a significant change in the distributions of streamlines and isotherms, compared to the base fluid. This change would be more important by considering Brownian motion. Indeed, Fig.11 portrays the developments of streamlines in the channel, with and without nanoparticles. It is seen that the streamlines plotted in Fig. 11 indicate that the primary recirculation zone behind the backward-facing step further shrinks, with nanoparticles. Meanwhile, the re-separation point of main flow moves upstream, as the main flow passes the backward-facing step, especially by considering the Brownian motion, and the recirculation zone neighboring to the step is evidently compressed. The results in Fig. 12 show that, in the region near the lower channel wall, the isotherms become more and more compact and approach to the bottom left corner of the channel. Therefore, it is reasonably expected that the heat transfer characteristics in this region can be effectively promoted as nanoparticle volume concentration increases. The effect of nanoparticles in the enhancement of the heat transfer becomes more important by considering the Brownian motion

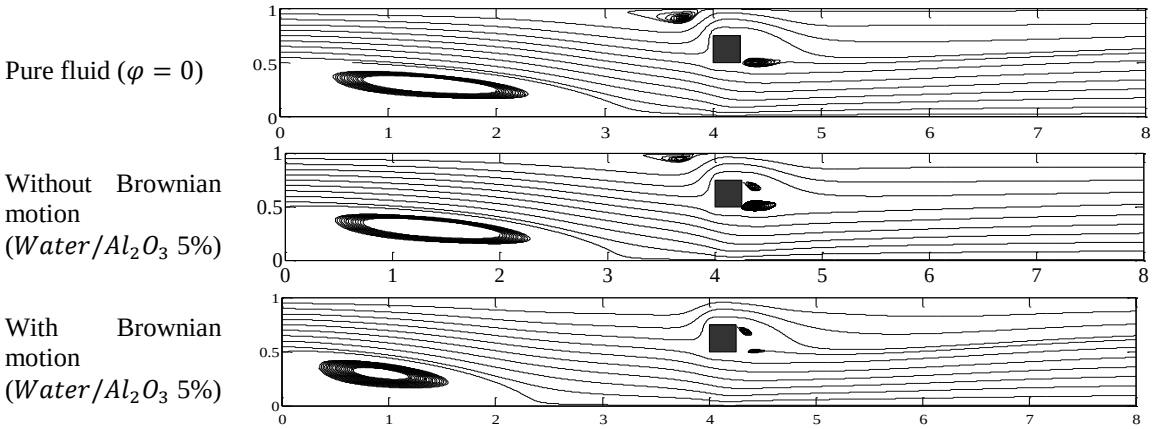

Figure 11. Flow pattern with square cylinder for $\mathrm{Water/Al_2O_3}$ nanofluid

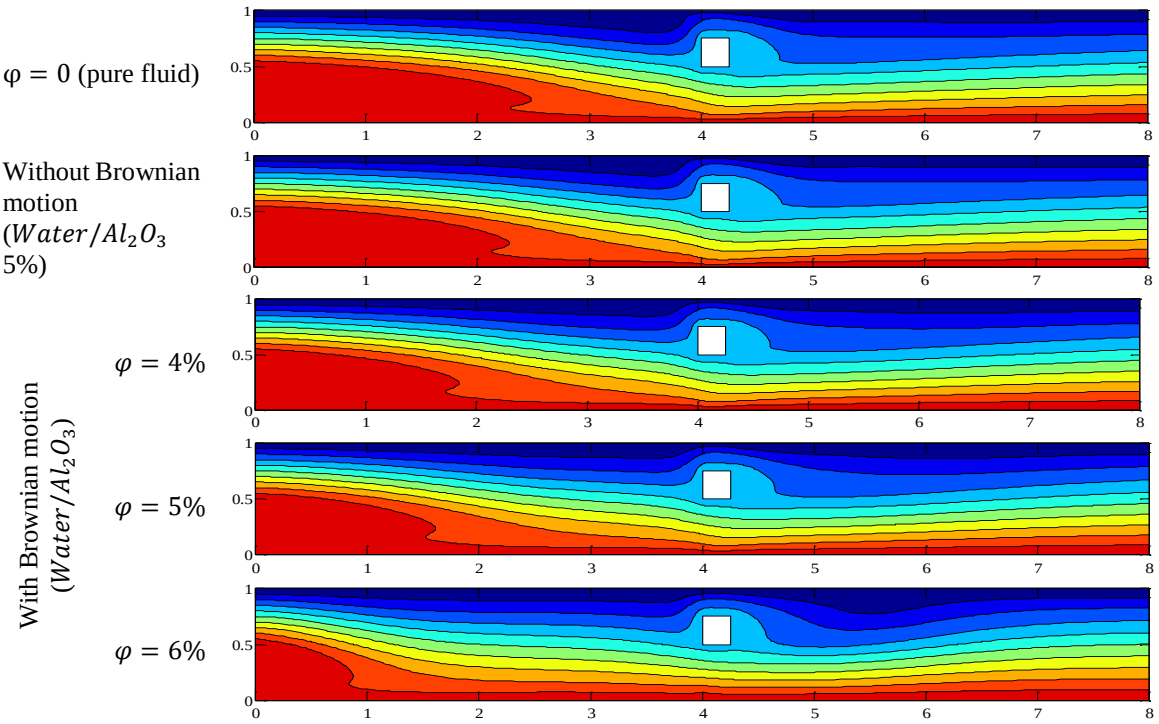

Figure 12. Isotherm contours for differents nanoparticles volume fraction for $Water/Al_2O_3$ nanofluid (with square cylinder)

Figure 13 presents the averaged Nusselt number at the lower and the upper walls in presence of square cylinder. This figure reveals a clear increase in the Nusselt number observed when increasing the nanoparticles volume fraction, up to 0.05, for different nanofluids, with and without square cylinder. Furthermore, as shown in this figure, the heat transfer increases in presence of square cylinder. As it can be seen, the Brownian motion has a significant effect on heat transfer in the presence of the square cylinder, where an important enhancement except on the lower wall was observed. Indeed, for $\varphi = 0.04$, we observe an increase of the heat transfer by 17.14%, 16.69% and 15.84%, for CuO, $Al_2O_3$and ZnO, respectively at the lower wall, compared with the one obtained without square cylinder.

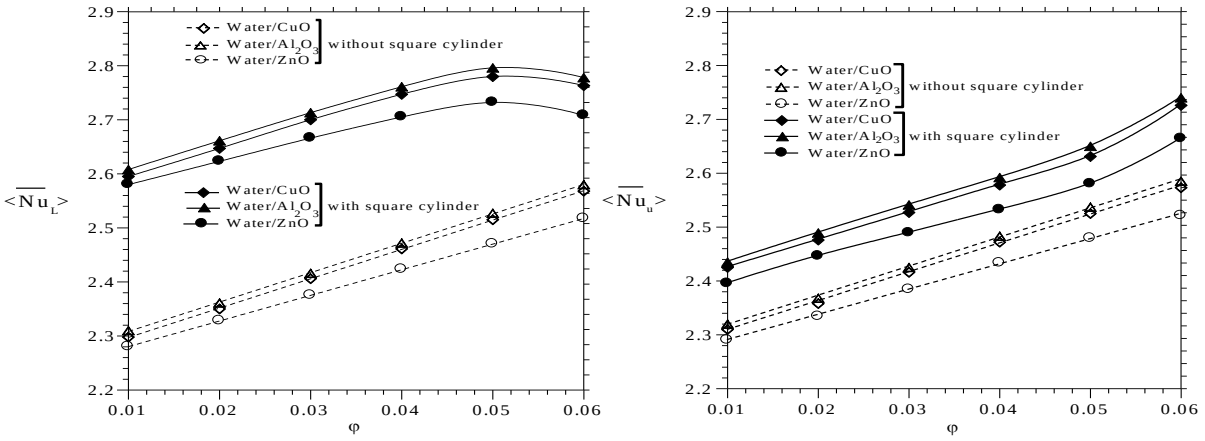

(a) : Lower wall (b) : Upper wall

Figure 13. Effect of square cylinder (with Brownian motion) on variation of $< \overline{Nu} >$ with φ

5. Conclusions

A numerical simulation has been done to study the effect of Brownian motion on the flow field and its related heat transfer of nanofluids over a backward-facing step with and without adiabatic square cylinder placed behind the first primary recirculation zone. Results obtained in the present study can be summarized as follows:

- The reattachment length decreases by adding nanoparticles to the base fluid. This reduction is in the vicinity of 7% and 64% in cases without and with Brownian motion, respectively, for a concentration of 0.06.
- The recirculation size decreases by considering Brownian motion.
- By considering the role of Brownian motion, without square cylinder, there is always an enhancement in heat transfer on the horizontal walls. However, the enhancement is more pronounced at high volume fraction of nanoparticles.
- The peaks of the maximum and minimum of the Nusselt number increases and moves towards at the inlet of channel by adding nanoparticles then by considering Brownian motion.
- The presence of adiabatic square cylinder is effective in augmenting the heat transfer. The results show that the heat transfer reaches its maximum at the emplacement of the square cylinder.
- With Brownian motion, the time average Nusselt number increases by increase in solid volume fraction less to 0.05 for all nanofluids. For example,for $\varphi = 0.04$, this augmentation is in the vicinity of 4.91%, 4.48% and 3.76%, for CuO, Al_2O_3 and ZnO, respectively in the lower wall. In presence of square cylinder, this augmentation becomes 17.14%, 16.69% and 15.84%, for CuO, Al_2O_3 and ZnO
- For all nanofluids produced higher results compared to pure water and it is clear that Al_2O_3nanofluid has the highest Nusselt number, followed by CuO and ZnO respectively.

Nomenclature

C_p	specific heat at constant pressure ($kJ.kg^{-1}.K^{-1}$)	x	dimensionless horizontal coordinate
h	convection heattransfer coefficient ($W.m^{-2}.K^{-1}$)	y	dimensionless vertical coordinate
H	downstreamchannelheight (m)	***Greek symbols***	
k	thermal conductivity ($W.m^{-1}.K^{-1}$)	α	thermal diffusivity ($m^2.s^{-1}$)
L	length of the channel (m)	β	coefficient of thermal expansion (K^{-1})
Lr	reattachmentlength, dimensionless	ϕ	transport quantity
Nu	Nusselt number	φ	nanoparticle volume fraction
$<\overline{Nu}>$	Time and space-average Nusselt number	ν	kinematicviscosity ($m^{-2}.s^{-1}$)
P	dimensionless pressure	μ	dynamic viscosity ($kg.m^{-1}.s^{-1}$)
p	pressure ($N.m^{-2}$)	θ	dimensionlesstemperature
Pe	Pecletnumber ($= Re.Pr$)	ρ	density ($kg.m^{-3}$)
Pr	Prandtl number ($=\frac{\nu_f}{\alpha_f}$)	τ	time dimensionalized
qw	heat flux at the wall ($W.m^{-2}$)	***Subscripts***	
Re	Reynolds number ($=\frac{\rho_f.u_0.H}{\mu_f}$)	av	average value
Ri	Richardson number ($=\frac{g.\beta_f.H^3.(T_h-T_c)}{\nu_f^2.R_e^2}$)	b	bulk value
T	dimensionaltemperature (K)	nf	Nanofluid
t	time non-dimensionalized (s)	f	fluid
x	meanchannelinletvelocity	s	solid
u_0	maximum velocity of the channel inlet	w	wall
u	dimensionless component of velocity	wc	cold wall
v	dimensionless y component of velocity	wh	hot wall
		av	average value
		b	bulk value

6. REFERENCES

1. B.F. Armaly, F. Durst, J.C.F. Pereira and B. Schönung, Experimental and theoretical investigation of backward-facing step flow, *J. Fluid Mech*., 1983, Vol. 127, P. 473–496.

2. M. Ramsak and L.A. kerget, Subdomain boundary element method for high-Reynolds laminar flow using stream function–vorticity formulation, *International Journal for Numerical Methods in Fluids*, 2004, Vol. 46, P. 815–47.

3. C. E., Tinney and E. L. S. Ukeiley, A study of a 3-D double backward-facing step, *Experiments in Fluids*, 2009, Vol. 47, P. 427–439

4. H. I. Abu-Mulaweh, A Review of Research on Laminar Mixed Convection Flow Over Backward and Forward-Facing Steps, *International Journal of Thermal Sciences*, 2003, Vol. 42, P. 897–909.

5. E. Abu-Nada, Application of nanofluids for heat transfer enhancement of separated flows encountered in a Backward Facing Step, *International Journal of Heat and Fluid Flow*, 2008, Vol. 29, P. 242–249.

6. A. Sh. Kherbeet, H.A. Mohammed and B. H. Salman, the effect of nanofluids flow on mixed convection heat transfer over microscale backward-facing step, *International Journal of Heat and Mass Transfer*, 2012, Vol. 55, P. 5870–5881.

7. H. A. Mohammed, O. A. Alawi and M.A. Wahid, Mixed convective nanofluid flow in a channel having backward-facing step with a baffle, *Powder Technology*, 2015, Vol. 275, P. 329–343.

8. T. Hussein, Laminar CuO–water nano-fluid flow and heat transfer in a backward-facing step with and without obstacle, *Applied Nanoscience*, 2015, DOI 10.1007/s13204-015-0441-7

9. K. Khanafer, K. Vafai and M. Lightstone, Buoyancy-driven heat transfer enhancement in a two-dimensional enclosure utilizing nanofluids, *International Journal of Heat and Mass Transfer*,2003, Vol. 46, P. 3639–3653.

10. F. P. Incropera and D. P. DeWitt, Fundamentals of Heat and Mass Transfer, 5th edn, 2007.

11. R. S. Vajjha, D. K. Das and D. P. Kulkarni, Development of new correlations for convective heat transfer and friction factor in turbulent regime for nanofluids, *International Journal of Heat and Mass Transfer*, 2010, Vol. 53, P. 4607-4618.

12. N. Masoumi, N. Sohrabi and A. Behzadmehr, A new model for calculating the effective viscosity of nanofluids, *J. Phys. D. Appl. Phys*., 2009, Vol. 42, No. 5, 055501.

13. R. S. Vajjha and D. K. Das, Experimental determination of thermal conductivity of three nanofluids and development of new correlations, *International Journal of Heat and Mass Transfer*, 2009, Vol. 52, P. 4675-4682

14. J. Koon and C. Kleinstreuer, A new thermal conductivity model for nanofluids, *Journal of Nanoparticle Research*, 2004, Vol. 6, No. 6, P. 577-588.

15. H. C. Brinkman, The viscosity of concentrated suspensions and solutions, *Journal of Chemical Physics*, 1952, Vol. 20, P. 571–581.

16. A. Sohankar, C. Norberg and L. Davidson, Low-Reynolds number flow around a square cylinder at incidence: Study of blockage, onset of vortex shedding and outlet boundary condition, *International Journal for Numerical Methods in Fluids*, 1998, Vol. 26, P. 39-56.

17. H. Abbassi, S. Turki and S. Ben Nasrallah, Channel flow bluff-body: outlet boundary condition, vortex shedding and effects of buoyancy, *Computational Mechanics*, 2002, Vol. 28, P. 10-16.

18. S. V. Patankar, Numerical heat transfer and fluid flow, *Series in Computational Method inMechanics and Thermal Sciences*, Mac Graw hill., 1980

19. M.S. Valipoor, R. Masoodi, S. Rashidi, M. Bovand and M. Mirhosseini, A numerical study on convection around a square cylinder using $AL_2O_3 - H_2O$ nanofluid, *Thermal science*, 2014, Vol. 18, No. 4, P. 1305-1314.

20. H.A. Mohammed, A.A. Al-aswadi, M.Z. Yusoff , and R. Saidur, Buoyancy-assisted mixed convective flow over backward-facing step in a vertical duct using nanofluids, *Thermophysics and Aeromechanics*, 2012, Vol. 19, No. 1, P. 33–52.